Electronic Supporting Information

$CaY_2Al_4SiO_{12}:Ce^{3+}$, Mn^{2+}: A single component phosphor to produce high color rendering WLEDs with blue chip

QiuhongZhang,[a] Junhao Li,[a]* Wei Jiang,[a] Litian Lin,[a] Jianhong Ding,[a] Mikhail G. Brik,[b,c,d] Maxim S. Molokeev,[e,f,g] Haiyong Ni[a]* and MingmeiWu[h]*

a *Guangdong Province Key Laboratory of Rare Earth Development and Application, Institute of Rare Metals, Guangdong Academy of Sciences, Guangzhou 510651, China*

b *College of Sciences & CQUPT-BUL Innovation Institute, Chongqing University of Posts and Telecommunications, Chongqing, 400065, P. R. China*

c *Institute of Physics, University of Tartu, W. Ostwald Str. 1, Tartu 50411, Estonia*

d *Faculty of Science and Technology, Jan Dlugosz University, ArmiiKrajowej 13/15, PL-42200, Częstochowa, Poland*

e *RAS, Fed Res Ctr KSC SB, Kirensky Inst Phys, Lab Crystal Phys, Krasnoyarsk 660036, Russia*

f *Siberian Fed Univ, Krasnoyarsk 660041, Russia*

g *Far Eastern State Transport Univ, Dept Phys, Khabarovsk 680021, Russia*

h *School of Marine Sciences, Sun Yat-Sen University, Zhuhai 510275, P. R. China*

*** Corresponding authors.**

Email: 327481344@qq.com; nhygd@163.com; ceswmm@mail.sysu.edu.cn

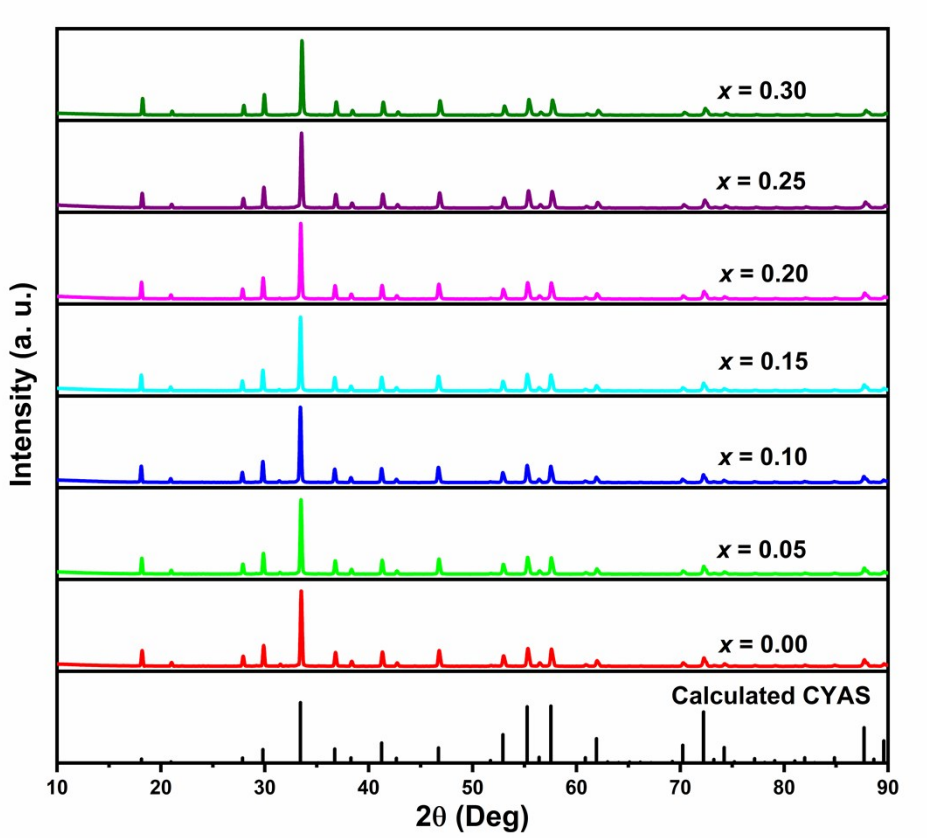

Fig. S1 XRD patterns of CYAS:0.02Ce, *x*Mn (*x* = 0.00 - 0.30) phosphors.

To determine the influence of Ce, Mn on the CYAS crystal structure, the phase purity of the prepared phosphors CYAS:0.02Ce, *x*Mn (*x* = 0.00 - 0.30) have been identified by powder XRD (Fig.S1, ESI). It is obvious that their diffraction peaks match well with the cubic CYAS, indicating that the addition of Ce and Mn ions did not change the main cubic crystal structure.

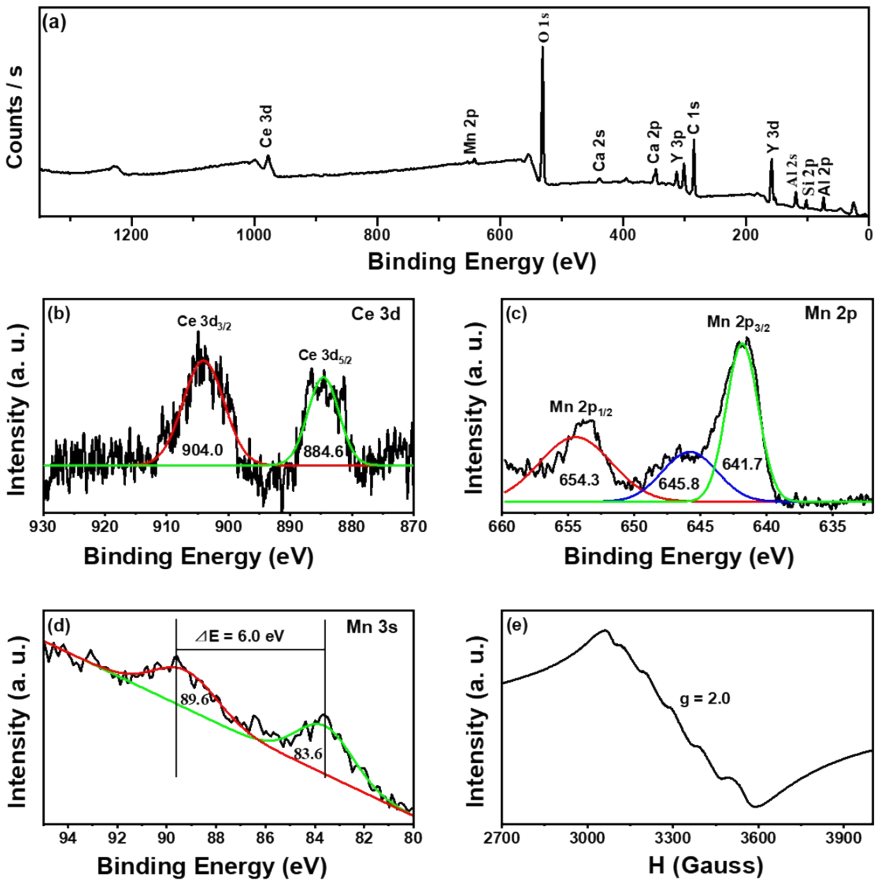

Fig. S2 (a) The survey scans XPS spectra of CYAS:0.02Ce, 0.30Mn phosphor.(b) High-resolution XPS spectra of Ce 3d, (c) Mn 2p and (d) Mn3s in CYAS:0.02Ce, 0.30Mn phosphor, and (e) EPR spectra of Mn in CYAS:0.02Ce, 0.05Mn phosphor.

To further investigate the valence state of the doped ions, the XPS spectra were studied. Fig.S2 (a) shows the survey scan XPS spectra of $Ca_{0.7}Y_{1.98}Al_4SiO_{12}$:0.02Ce, 0.3Mn phosphor. It clearly exhibits the signals from Al2p, Al2s, Si2p, O1s, Y3d, Ca2p, Ce3d and Mn2p, which indicates

the Mn and Ce ions were successfully introduced into the CYAS crystal lattice. Fig.S2 (b, c, d) shows the high-resolution XPS spectrum of Mn2p, Mn3s and Ce 3d. Mn2p shows two separate peaks $2p_{1/2}$ and $2p_{3/2}$ with binding energies at 653.5 eV and 641.7 eV, respectively (Fig.3b). XPS spectrum of Mn3s was collected to precisely determine the valence state of Mn ions. Accordingto the reported work, the valence of Mn (v_{Mn}) can be obtained from the energy of exchange splitting of the Mn3*s* spectra (ΔE_{3s}) based on the following linear equation: $\nu_{Mn} = 9.67 - 1.27\Delta E_{3s}$.[1] For our $Ca_{0.7}Y_{1.98}Al_4SiO_{12}$:0.02Ce, 0.3Mn sample, ΔE_{3s} was found to be about 6.0 eV, as shown in Fig.3(c), indicating that the manganese valence should be +2 oxidation state, as well as not the mixture with Mn^{3+} and Mn^{4+}. The Ce 3d shows two separate peaks in Fig.3(d) (binding energy $Ce3d_{3/2}$ at 904.0 eV and $Ce3d_{5/2}$ at 884.6 eV), which unambiguously attributed to the +3 oxidation state.

The EPR spectrum of $Ca_{0.7}Y_{1.98}Al_4SiO_{12}$:0.02Ce, 0.05Mn is shown in Fig.3e. The EPR spectrum shows six resolved hyperfine features at g = 2.0, which refer to the allowed interactions between electron (S = 5/2) and nuclear (I = 5/2) spins of the incorporated Mn^{2+} ions in the crystalline structure of CYAS host.

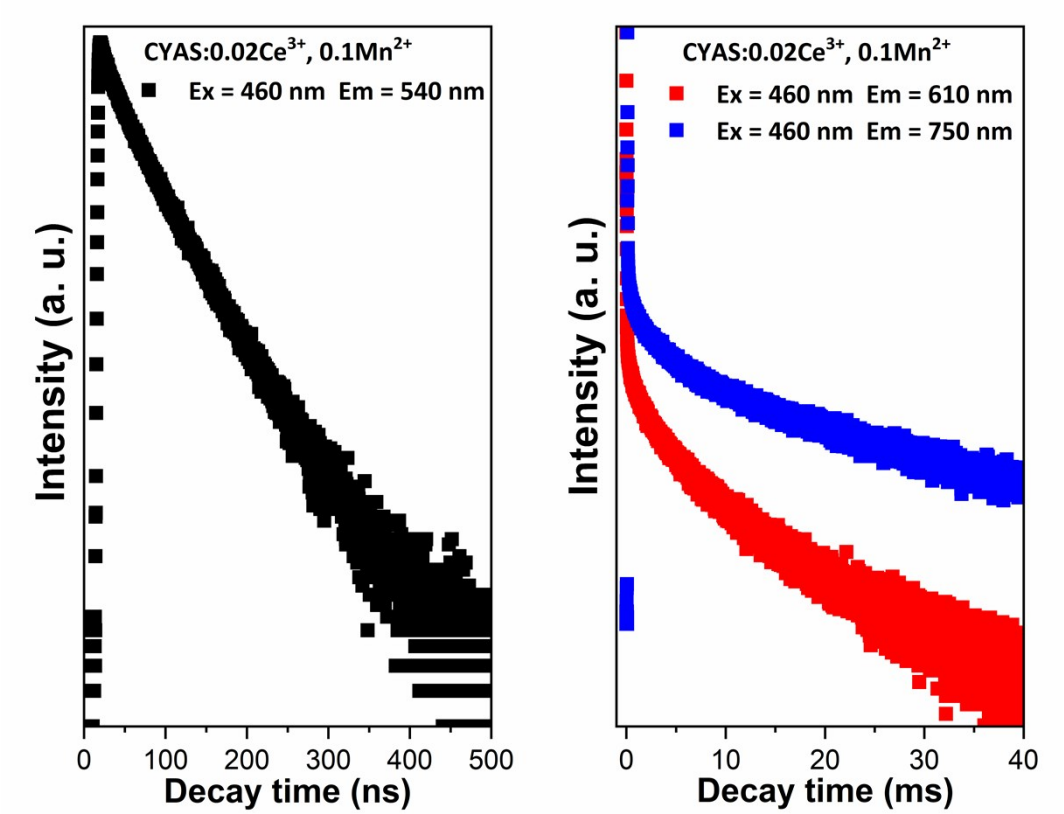

Fig. S3 The decay curves of 540 nm emission band (λ_{em} = 540 nm, λ_{ex} = 460 nm), 616 nm emission band (λ_{em} = 616 nm, λ_{ex} = 460 nm) and 750 nm emission band (λ_{em} = 750 nm, λ_{ex} = 460 nm) of CYAS:0.02Ce^{3+}, 0.10Mn^{2+}.

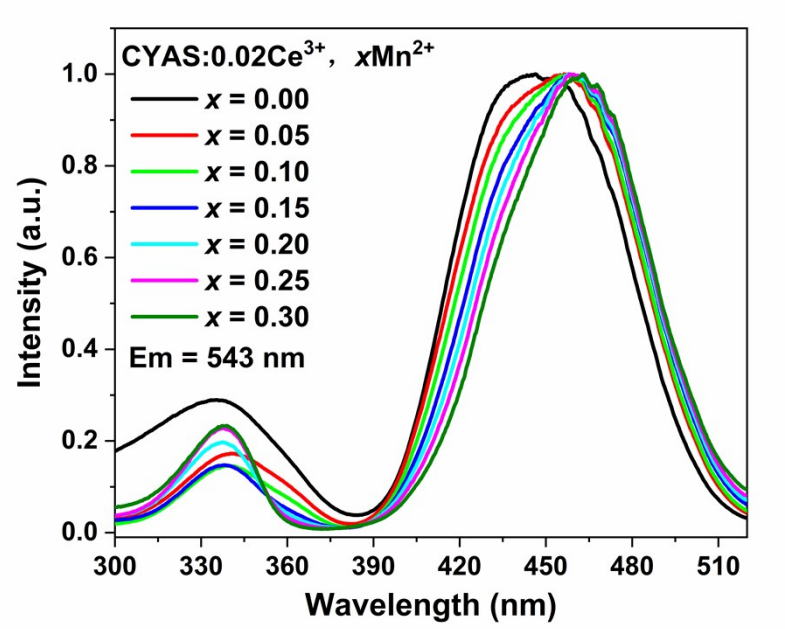

Fig. S4 Normalized PLE spectra of CYAS:0.02Ce, *x*Mn (*x* = 0.00 - 0.30) phosphors. (λ_{em} = 543 nm).

Monitoring at 543 nm emission, the normalized PLE spectra of CYAS: 0.02Ce^{3+}, *x*Mn^{2+} show two broad absorption bands in the range of 300-520 nm. The absorption bands exhibit red shift obviously with the introduction of the Mn^{2+}, but the absorption bands exhibit red shift slightly with the increasing of Mn^{2+} concentration. The red shift of the absorption bands are due to the Mn^{2+} ions replacing the bigger Ca^{2+}/Y^{3+} ions. The slight red shift with increasing Mn^{2+} concentration indicates that part of Mn^{2+} ions occupy smaller Al^{3+} ions. Therefore, at low doping concentration, Mn^{2+} ions tend to replace the Ca^{2+}/Y^{3+} ions, while the

Mn^{2+} ions gradually replace Al^{3+} ions with increasing Mn^{2+} concentration.

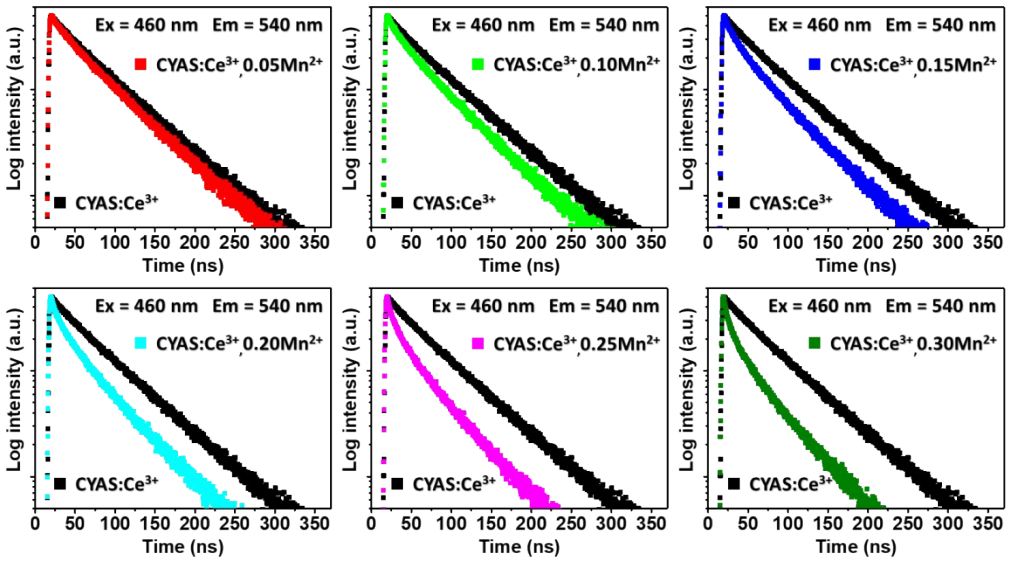

Fig. S5 Decay curves of Ce^{3+} in CYAS: 0.02Ce, *x*Mn (*x* = 0.00 - 0.30) phosphors (λ_{ex} = 460 nm, λ_{em} = 540 nm).

In order to further confirm whether the energy transfer between Ce^{3+} and Mn^{2+} exists, the decay curves of CYAS:0.02Ce^{3+}, *x*Mn^{2+} phosphors (*x* = 0.00 - 0.30) (λ_{ex} = 460 nm, λ_{em} = 540 nm) were measured and shown in (Fig.S5, ESI). The decay curve of the Ce^{3+}single doped sample is well fitted with a single-exponential decay mode. The decay curves of Ce^{3+} depart from the single-exponential decay mode for Mn^{2+} codoped samples due to the energy transfer. The decay times of Ce^{3+} in CYAS:0.02Ce, *x*Mn phosphors shortened with the increase of Mn^{2+} content (Table S1, ESI), confirming the possibility of energy transfer from Ce^{3+} to Mn^{2+} ions in CYAS host.

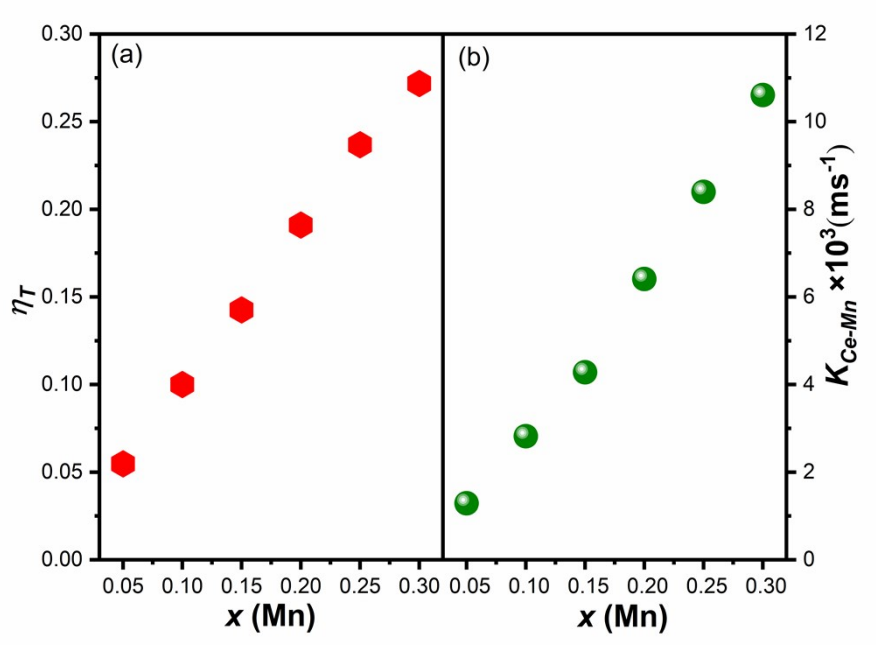

Fig. S6 Dependence of η_T and $K_{\text{Ce-Mn}}$ as function of x values in CYAS: 0.02Ce, xMn (x = 0.00 - 0.30) phosphors.

The energy transfer efficiency (η_T) from Ce^{3+} to Mn^{2+} can be expressed by equation (1) and the nonradiative energy-transfer rate from the excited state of Ce^{3+} to the matching energy level of Mn^{2+}can be expressed by equation (2)

$$\eta_T = 1 - \tau/\tau_0 \qquad (1)$$

$$K_{Ce-Mn} = 1/\tau - 1/\tau_0 \qquad (2)$$

where τ andτ_0 are the decay times of Ce^{3+} with and without Mn^{2+} presence. As shown in the (Fig.S6, ESI) and Table S1, the energy transfer efficiency η_T and the energy-transfer rate of Ce^{3+}-Mn^{2+} increase with the increase of Mn^{2+} concentrations, indicating that a much more efficient

energy-transfer process occurred in the high concentration Mn^{2+} doped YACS samples.

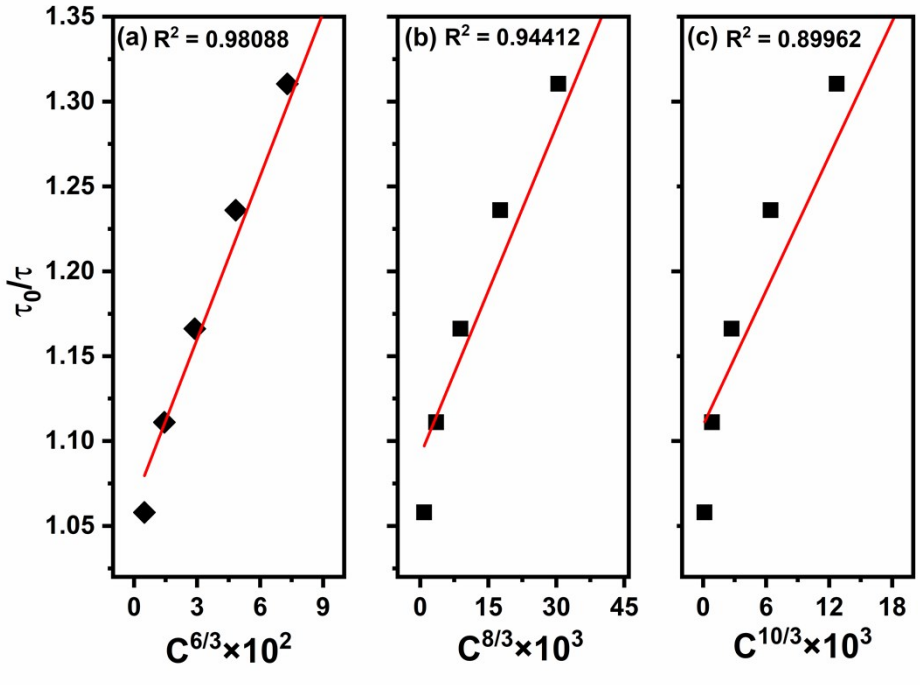

Fig. S7 Dependence of τ_0/τ of Ce^{3+} on (a)$C^{6/3}$, (b)$C^{8/3}$ and (c)$C^{10/3}$.

According to Dexter and Uitert, exchange interaction and multipolar-multipolar interaction might involve in the energy transfer between a sensitizer and an activator.[2-5] It is also known that the dominant interaction is strongly dependent on the separation between the sensitizer and activator. In order to confirm which interaction dominates the energy transfer between the Ce^{3+} and Mn^{2+} ions, we estimated the separation $R_{Ce\text{-}Mn}$ between Ce^{3+} and Mn^{2+} ions in CYAS:0.02Ce^{3+}, 0.30Mn^{2+} using the formula suggested by Blasse:[6]

$$R_{Ce-Mn} = 2\left(\frac{3V}{4\pi xN}\right)^{1/3} \quad (3)$$

where N is the number of molecules in the unit cell, V is the unit cell volume, and x is the total concentration of Ce^{3+} and Mn^{2+}. For CYAS:0.02Ce, 0.30Mn, V = 1712.99 $Å^3$, x = 0.02 + 0.30 = 0.32 and Z = 8. So the distance $R_{Ce\text{-}Mn}$ in CYAS:0.02Ce, 0.30Mn is estimated to be 10.85 Å. The multipolar-multipolar interaction corresponds to long range energy transfer, while the exchange interaction occurs only if the separation is short enough (R < 8 Å) to allow a direct overlap of their wave functions. Since the distance $R_{Ce\text{-}Mn}$ with the highest doping concentration is still larger than 8 Å, so the energy transfer between Ce^{3+} and Mn^{2+} in the prepared samples is not possible through exchange interaction. So we would like to suggest that the multipolar-multipolar interaction is dominant in the energy transfer between Ce^{3+} and Mn^{2+} in CYAS.

If the multipolar-multipolar interaction takes control, the lifetime of the sensitizer and the concentration of the activator should follow the formula:

$$\frac{\tau_0}{\tau} \propto C^{n/3} \qquad (4)$$

where C represents the total concentration of Ce^{3+} and Mn^{2+}, and n equals to 6, 8 and 10, corresponding to dipole-dipole, dipole-quadrupole, and quadrupole-quadrupole interactions, respectively. In order to indentify the energy transfer mechanism from Ce^{3+} to Mn^{2+} in CYAS, the τ_0/τ–$C^{n/3}$ plots are depicted in Fig.S6. It is apparent that the curve is best close to

the linear relation when n = 6, which indicates that dipole-dipole interaction was dominated the energy transfer from Ce^{3+} to Mn^{2+} ions in CYAS.

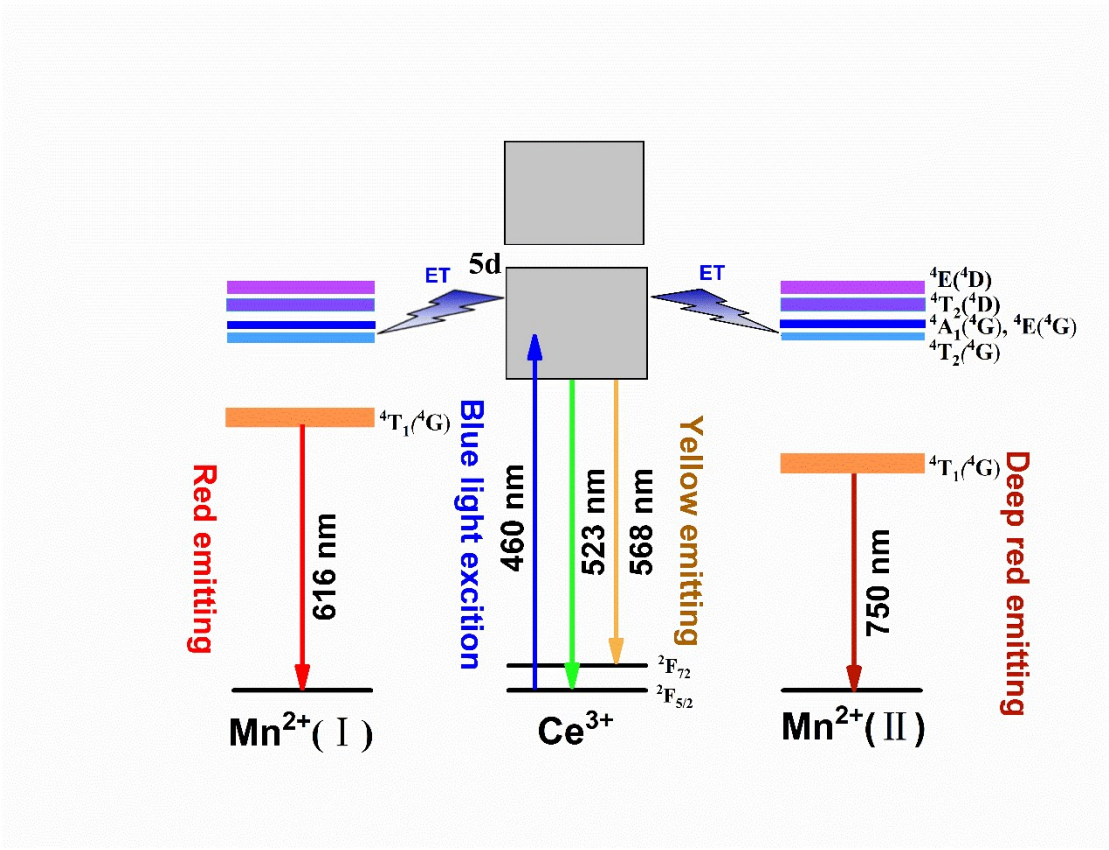

Fig. S8 The schematic diagram of energy transfer between Ce^{3+}-Mn^{2+} in CYAS.

Upon 460 nm blue light excitation, Ce^{3+} is excited from the ground state to the 5d state, and the yellow emission can be observed due to the 5d-4f transitions of Ce^{3+}. Part of the energy absorbed by the sensitizer Ce^{3+} efficiently transfers to Mn^{2+} through a dipole-dipole interaction, the emission intensity of Mn^{2+} at 616 nm and 750 nm is enhanced. Finally the yellow, red and deep red emission can be simultaneously observed in CYAS host.

Table S1 The decay times of Ce^{3+} (τ), energy transfer efficiency (η_T) and energy transfer efficiency and rate ($K_{Ce\text{-}Mn}$) from Ce^{3+} to Mn^{2+} in CYAS:0.02Ce^{3+}, $x$$Mn^{2+}$ (x = 0.00 - 0.30) phosphors.

x	0.00	0.05	0.10	0.15	0.20	0.25	0.30
τ(ns)	80.11	75.72	72.10	68.69	64.81	61.13	58.34
η_T (%)	-	5.48	10.00	14.26	19.10	23.69	27.18
$K_{Ce\text{-}Mn}\times10^3$(ms^{-1})	-	0.72	1.39	2.08	2.95	3.88	4.66

References

1 E.Beyreuther, S.Grafströmand M. L.Eng, *Phys. Rev. B*, 2006, ***73***,155425.

2 C.H. Huang and T.M. Chen, *Opt. Express*, 2010, **18**, 5089-5099.

3 D.L. Dexter, *J. Chem. Phys.*, 1953, **21**, 836-850.

4 L.G. Van Uiter, *J. Electrochem. Soc.*, 1967, **114**, 1048-1053.

5 M.M. Shang, C.X. Li and J. Lin, *Chem. Soc. Rev.*, 2014, **43**, 1372-1386.

6 G. Blasse, *Phys. Lett. A*, 1968, **28**, 444-445.